

**This is an electronic reprint of the original article.
This reprint *may differ* from the original in pagination and typographic detail.**

Author(s): Laulainen, Janne; Kalvas, Taneli; Koivisto, Hannu; Kronholm, Risto; Tarvainen, Olli; Aleiferis, S.; Svarnas, P.

Title: Photoelectron emission experiments with ECR-driven multi-dipolar negative ion plasma source

Year: 2017

Version:

Please cite the original version:

Laulainen, J., Kalvas, T., Koivisto, H., Kronholm, R., Tarvainen, O., Aleiferis, S., & Svarnas, P. (2017). Photoelectron emission experiments with ECR-driven multi-dipolar negative ion plasma source. In D. Faircloth (Ed.), NIBS 2016 : Fifth International Symposium on Negative Ions, Beams and Sources (Article 020012). AIP Publishing. AIP Conference Proceedings, 1869. <https://doi.org/10.1063/1.4995718>

All material supplied via JYX is protected by copyright and other intellectual property rights, and duplication or sale of all or part of any of the repository collections is not permitted, except that material may be duplicated by you for your research use or educational purposes in electronic or print form. You must obtain permission for any other use. Electronic or print copies may not be offered, whether for sale or otherwise to anyone who is not an authorised user.

Photoelectron emission experiments with ECR-driven multi-dipolar negative ion plasma source

J. Laulainen, T. Kalvas, H. Koivisto, R. Kronholm, O. Tarvainen, S. Aleiferis, and P. Svarnas

Citation: [AIP Conference Proceedings](#) **1869**, 020012 (2017); doi: 10.1063/1.4995718

View online: <http://dx.doi.org/10.1063/1.4995718>

View Table of Contents: <http://aip.scitation.org/toc/apc/1869/1>

Published by the [American Institute of Physics](#)

Articles you may be interested in

[VUV emission spectroscopy combined with \$H^-\$ density measurements in the ion source Prometheus I](#)
AIP Conference Proceedings **1869**, 030045 (2017); 10.1063/1.4995765

[Experimental study of H atom recombination on different surfaces in relation to \$H^-\$ negative ion production](#)
AIP Conference Proceedings **1869**, 020011 (2017); 10.1063/1.4995717

[Spectroscopic study of molecular hydrogen concentration at the vicinity of metal surfaces](#)
AIP Conference Proceedings **1869**, 020010 (2017); 10.1063/1.4995716

[Negative ion formation from a low-work-function nanoporous inorganic electride surface](#)
AIP Conference Proceedings **1869**, 020005 (2017); 10.1063/1.4995711

[Extraction layer models for negative ion sources](#)
AIP Conference Proceedings **1869**, 020006 (2017); 10.1063/1.4995712

[Study of negative hydrogen ion production at low work function material surface using a hydrogen atom source](#)
AIP Conference Proceedings **1869**, 020009 (2017); 10.1063/1.4995715



SUMMER SALE!

30% OFF
ALL PRINT
PROCEEDINGS!

AIP | Conference Proceedings

ENTER COUPON CODE
SUMMER2017

Photoelectron Emission Experiments with ECR-driven Multi-dipolar Negative Ion Plasma Source

J. Laulainen^{1,a)}, T. Kalvas¹, H. Koivisto¹, R. Kronholm¹, O. Tarvainen¹,
S. Aleiferis² and P. Svarnas²

¹*University of Jyväskylä, Department of Physics, Finland*

²*High Voltage Laboratory, Department of Electrical and Computer Engineering, University of Patras, Rion-Patras
26504, Greece*

^{a)}Corresponding author: janne.p.laulainen@student.jyu.fi

Abstract. Photoelectron emission measurements have been performed using a 2.45 GHz ECR-driven multi-dipolar plasma source in a low pressure hydrogen discharge. Photoelectron currents induced by light emitted from ECR zone and H⁻ production region are measured from Al, Cu, Mo, Ta, and stainless steel (SAE 304) surfaces as a function of microwave power and neutral hydrogen pressure. The total photoelectron current from the plasma chamber wall is estimated to reach values up to 1 A for 900 W of injected microwave power. It is concluded that the volumetric photon emission rate in wavelength range relevant for photoelectron emission is a few times higher in arc discharge.

INTRODUCTION

It has been theoretically shown that in low temperature hydrogen plasmas at least 10% of heating power is dissipated via photon emission when at least 1% of the heating power is dissipated in ionization [1]. It has also been demonstrated experimentally that a significant fraction of plasma heating power is dissipated via vacuum ultraviolet (VUV) emission in arc discharge [2], ECR [3] and RF hydrogen plasmas [4]. Photons in the VUV range (wavelength < 150 nm) carry enough energy to induce a significant emission of photoelectrons (PE) when they impinge on a metal surface (typical work function 4–5 eV) on the plasma chamber wall [5]. Additional electrons produced by PE emission might have a considerable effect on plasma properties and especially on the formation of the plasma sheath. PE emission measurements with a filament driven hydrogen arc discharge ion source ‘LIISA’ have been reported earlier in Ref. [5]. In this paper PE emission measurements with the ECR-driven multi-dipolar plasma source ‘Prometheus I’ are reported and the results are compared to those obtained from the arc discharge.

A major difference between arc discharges and ECR discharges is the electron energy distribution (EED). In arc discharge plasmas, the EED spans from very low energies up to the energy corresponding to the cathode bias forming a rather uniform distribution [6]. In ECR plasmas, the EED is often considered Maxwellian. Although, two electron populations with temperatures of 1–5 eV and ≥ 10 eV can typically be identified [7]. The EED might have a notable effect on PE emission as the volumetric dissociation rate through electronic excitation to triplet states depends strongly on the EED. The dissociation rate itself affects the atomic to molecular hydrogen fraction in the discharge and, therefore, plays a crucial role on plasma emission spectrum. Even small changes in the light emission spectrum might have a considerable effect on the PE emission since the quantum efficiency for common metals is heavily dependent on photon energy [8, 9]. PE emission is predominantly caused by Lyman-alpha and Werner-band emission, because the quantum efficiency of common metals increases in the VUV range with decreasing wavelength of the incident radiation. The dissociation rate has been observed to be considerably higher in microwave-driven ion sources [3], whereas the EED in arc discharge leads to dominance of molecular excitation.

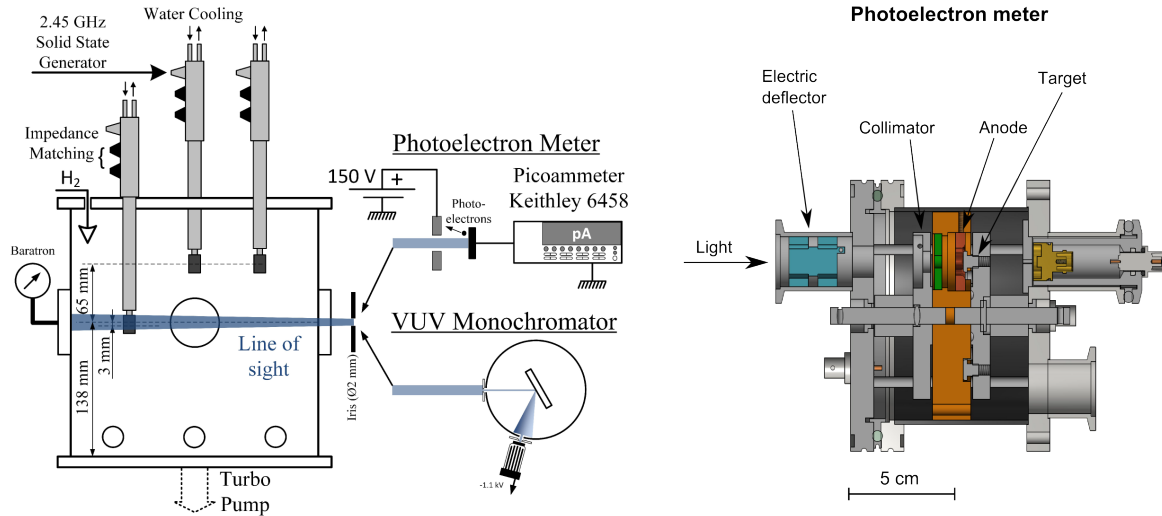


FIGURE 1. Setup for photoelectron emission measurements with ‘Prometheus I’ ion source and details of the photoelectron meter.

MEASUREMENT SETUP

The experimental setup is presented in Figure 1. The experimental data presented in this article were taken with the ECR-driven multi-dipolar plasma source Prometheus I [10] in a low pressure hydrogen discharge. The plasma is sustained by a 2D network of ECR plasma sources [11, 12]. Each elementary source consists of two parts: a cylindrical samarium-cobalt ($\text{Sm}_2\text{Co}_{17}$) permanent magnet, magnetized along its axis, and a coaxial line parallel to the magnetization vector, with an open end at the rear of the magnet. The sources are driven individually at 2.45 GHz by five solid state power supplies (0–180 W/elementary source). A tuner embedded on the main body of each source is used for impedance matching in order to minimize microwave power reflection (maximum accepted reflected power of 5 W). A turbo-molecular pump adapted under the bottom flange pumps the source down to $2 \cdot 10^{-6}$ Torr. High purity hydrogen is introduced by a digital mass flow controller (MKS 1179B) from the top flange to obtain a working pressure between 1 and 20 mTorr. The pressure is accurately monitored with an absolute pressure transducer (MKS Baratron 627D). The cubic plasma chamber (24 cm edge) is made from stainless steel (SS), and the central viewport that was used in the studies is located 138 mm above the bottom of the chamber.

The magnetic field of the source plays two roles for the application of negative ion production. Firstly, the necessary resonance zone with 875 G magnetic field intensity is created to satisfy the ECR condition. The ECR zone of Prometheus I is depicted in Ref. [10]. The second function is to confine hot electrons in the vicinity of the magnets

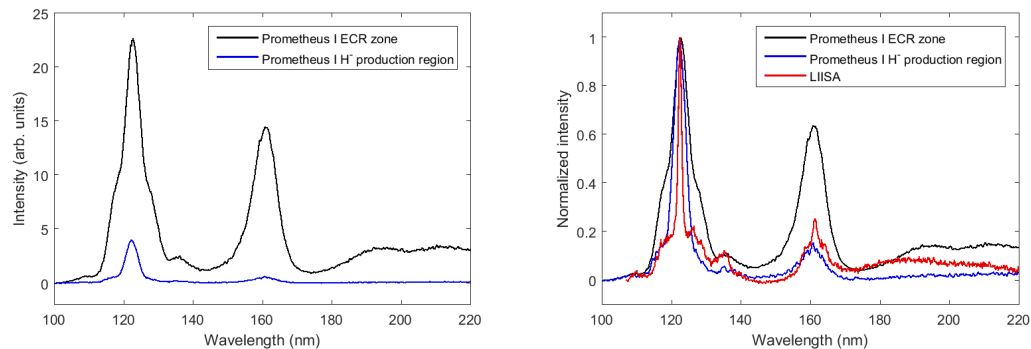


FIGURE 2. Measured VUV spectra of hydrogen plasmas in ‘Prometheus I’ and ‘LIISA’ ion sources.

and, in this respect, work as the magnetic filter of the source. The elementary sources are vertically movable, and in the experiments the source was used in two configurations. In the first, the photoelectron meter is looking to the H^- production region, 65 mm below the midplane of the ECR zones. In the second, the meter is looking to the ECR zones, 3 mm above the midplane of the ECR zones.

The spectra of the hydrogen plasma was measured from the central viewport in both configurations in order to obtain fundamental information of the VUV emission. In Figure 2, the VUV spectra measured from Prometheus I is presented and, for comparison, a corresponding spectrum from LIISA is also plotted. The apparent broadening of the Prometheus I VUV spectra in comparison to the one measured from the LIISA ion source is due to the different measurement geometry. In the case of Prometheus I the distance from the plasma to the entrance slit of the monochromator is 28 cm, which is significantly less than in the case of LIISA (1.5 m). Moreover, the light emission from the LIISA ion source is collimated by the extraction aperture far from the monochromator entrance slit as described in Ref. [2] whereas the iris in Prometheus I setup is located in the close proximity of the slit. Hence, the angular spread of the photons incident on the monochromator is larger for the Prometheus I setup, which results to decreased wavelength resolution of the VUV spectrum. The geometrical effects of the light source on VUV spectroscopy are described thoroughly in Ref. [13]. In the ECR zone, the electron temperature is higher, which results to higher Lyman-band and Werner-band emission compared to the H^- production region. In the H^- production region, Lyman-alpha dominates, which indicates higher dissociation degree compared to the ECR zone. In the ECR discharge, the EED has to be determined locally, since the heating power is dissipated to the plasma predominantly on the ECR surface and, consequently, the hot electron density is higher in the ECR zone. In arc discharge with a good magnetic confinement, plasma is heated more evenly by the thermally emitted electrons. A parametric study of VUV emission in Prometheus I is reported in Ref. [14].

The photoelectron meter is described in detail in Ref. [5]. Its cross sectional view is presented in Figure 1. On the first disc facing the plasma, a 2 mm collimator was adapted to limit the photon flux incident on the sample. The light that passes the collimator illuminates the sample (photocathode) which is grounded through a picoammeter (Keithley 6458) measuring the PE current. The sample is placed 120 mm away from the chamber wall or 240 mm away from the center of the ECR zone. The emitted electrons are collected with an anode ring located approximately 3 mm from the target and biased to +150 V with respect to the cathode i.e. laboratory ground. An aluminium plate, adapted on the first rotating disc, protects the sample from the VUV light when measurements are not being made. Samples are cleaned in atmospheric pressure, but they are covered with their natural oxides, which can give rise to VUV induced surface modification that can change the PE emission [15]. The measurements are performed in ion source relevant conditions, and within two hours of exposure the measured PE current was observed to vary less than 6%. The sample, which is adapted on a second rotating disc, can be changed during measurements without compromising the vacuum in order to study different materials. A parametric study is realized with materials typically used in negative hydrogen

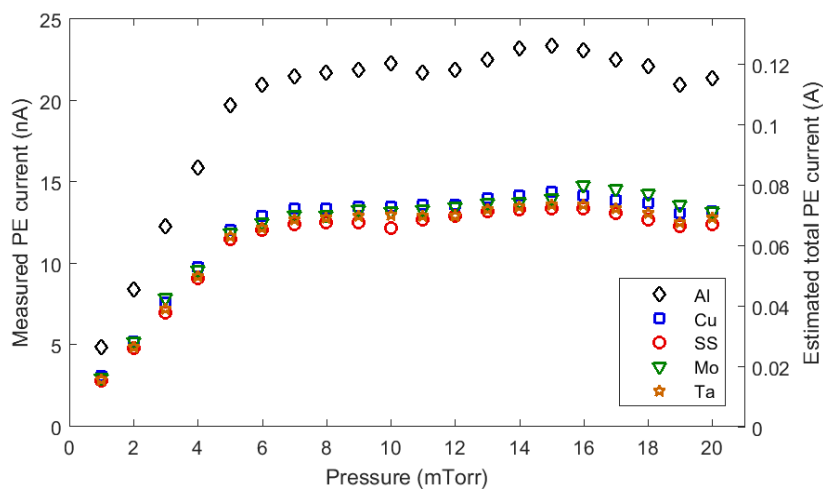


FIGURE 3. Photoelectron currents from different metal samples when the photoelectron meter is looking to the H^- production region. The power is maintained constant at 900 W (180 W/elementary source) and the pressure is varied.

ion sources as chamber materials (Al, Cu, SS) [16, 17, 18], filament materials (Ta) [19, 20], plasma grid materials (Mo) [21] or so-called collar materials (SS, Mo) [22, 23].

In the photoelectron meter, photons strike the sample with normal incidence whereas, in actual discharge chamber their angle of incidence covers a large solid angle. The mean free path for 10 eV VUV photons, corresponding to the dominant Lyman-alpha emission of hydrogen plasmas, varies in the range of 8–13 nm for the materials used in this study [24] while typical escape depth of photoelectrons is 1–3 nm [25]. Because the penetration depth of the photons exceeds the electron escape depth, it could be expected that the angle of incidence affects the quantum efficiency of the photoelectron emission at Lyman-alpha wavelength. However, it was confirmed with atomic-force microscopy that the peak-to-peak roughness of the sample surface exceeds 100 nm, which effectively randomizes the photon angle of incidence. Similar to the samples manufactured for this work, technical surfaces in ion sources are rough in the nanoscale and, thus, it is concluded that angular effects in photoelectric yield are probably insignificant in this case.

EXPERIMENTAL RESULTS

The measured PE emission and estimated total PE emission for Al, Cu, SS (SAE 304), Mo, and Ta samples for both source configurations is presented in Figures 3–6. In Figures 3 and 5, the variation of the PE current as a function of the filling gas pressure is plotted, while the power is maintained constant at 900 W (180 W/elementary source). In Figures 4 and 6, the PE current from all the samples is presented as a function of the microwave power per elementary source for four selected pressures. Much more light is emitted from the ECR zone compared to H⁻ production region and, thus, there is almost an order of magnitude difference in PE emission. The PE currents measured from Cu, SS, Mo, and Ta are approximately equal while the signal from Al is consistently about 50% higher. The fact that Al always has the highest PE current is most probably due to higher quantum efficiency in the VUV range.

The line-of-sight plasma volume covers only a few percent of the total plasma chamber volume. In order to estimate the total PE current from the internal surface of Prometheus I, the measurements need to be extrapolated.

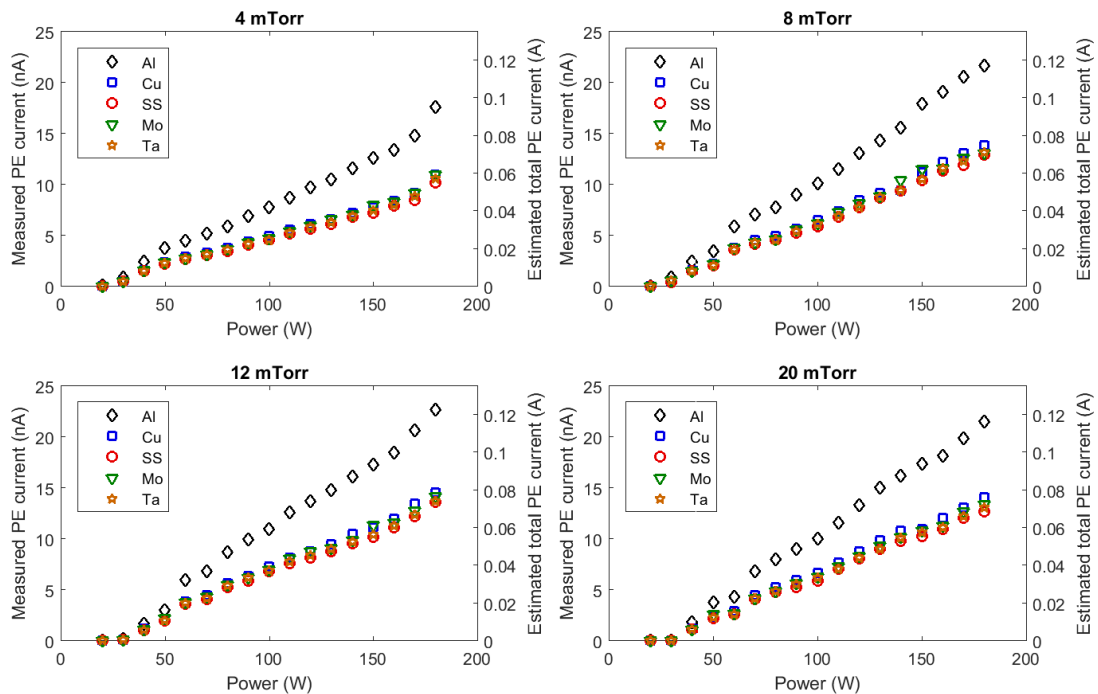


FIGURE 4. Photoelectron currents from different metal samples when the photoelectron meter is looking to the H⁻ production region. The power is varied in selected pressures.

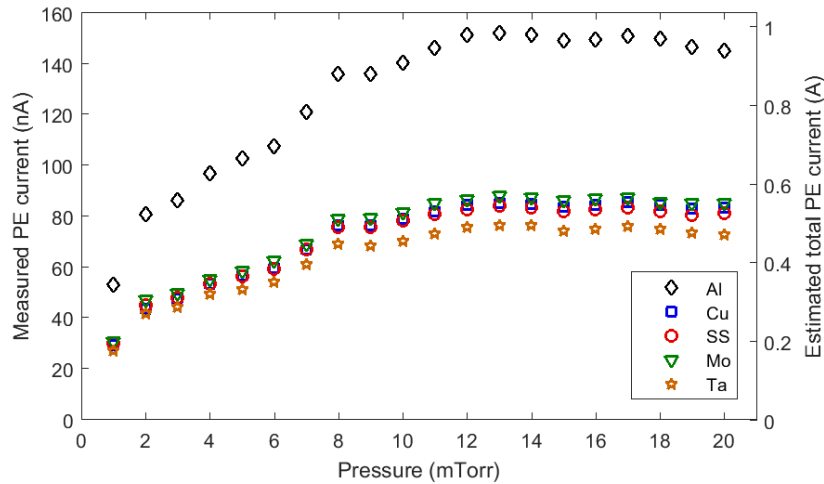


FIGURE 5. Photoelectron currents from different metal samples when the photoelectron meter is looking to the ECR zone. The power is maintained constant at 900 W (180 W/elementary source) and the pressure is varied.

Monte Carlo methods were used to calculate the probability for a single photon to reach the target surface. The total PE current is obtained by dividing the measured current with the given probability. In the simulations, the light emission profile is assumed homogeneous and isotropic across the plasma chamber profile. In reality, the spatial distribution of the plasma light emission rate depends on the inhomogeneous plasma density and temperature profiles. Without accurate information about the density and temperature profiles in the entire plasma volume the total PE flux can only be estimated. However, in the H^- production region, the plasma properties (as measured with a horizontally movable probe) show only low variation along the source width (typically: cold electron density 25%, cold electron temperature 15%, plasma potential 2%, and floating potential 15%) [26]. The estimated total PE current for the H^- production region is in the order of 0.1 A, which can be considered as the lower limit for the total PE emission. The estimated total PE emission reaches values of 1 A, when the ECR zone is in the line-of-sight, and this can be considered as a possible maximum current. The lower and upper limits are obtained assuming that the whole plasma chamber volume emits light corresponding to H^- production region and ECR zone, respectively.

DISCUSSION

It has been estimated from the measured data that the maximum PE current from the total internal surface of Prometheus I is on the order of 1 A for 900 W of injected microwave power. Taking into account the surface area of the Prometheus I plasma chamber this corresponds to PE emission of 0.3 mAcm^{-2} per kW. This value can be compared to the previous measurement with the arc discharge source LIISA in which the PE current density is estimated to be three times higher for the same total power [5]. On the other hand, based on the PE measurements, the volumetric photon emission rate in wavelength range relevant for PE emission is concluded to be five times higher in the arc discharge. This indicates that the power efficiency is better in arc discharge compared to ECR discharge. However, the PE flux from the wall to the plasma is limited by the cusp magnetic field of LIISA, since the cross field diffusion of the emitted electrons in transverse magnetic field is significantly slower than their propagation along the field lines. In Prometheus I, the transverse magnetic field intensity is lower near the plasma chamber walls, and the emitted electrons are accelerated towards the plasma by the positive plasma potential. Secondary electron emission can be considered insignificant in comparison to PE emission, since the secondary electron emission yield is small for low energy electrons [27]. In Prometheus I, high energy electrons are captured near the ECR zone due to the magnetic field and electrons escaping from the plasma are also decelerated by the positive plasma potential.

The role of additional electrons to the plasma properties depends strongly on the energy of the electrons. Photoelectrons are emitted with all energies from zero up to the maximum energy, which corresponds to the difference between the energy of the absorbed photon and the surface work function. For common metals used in this study the

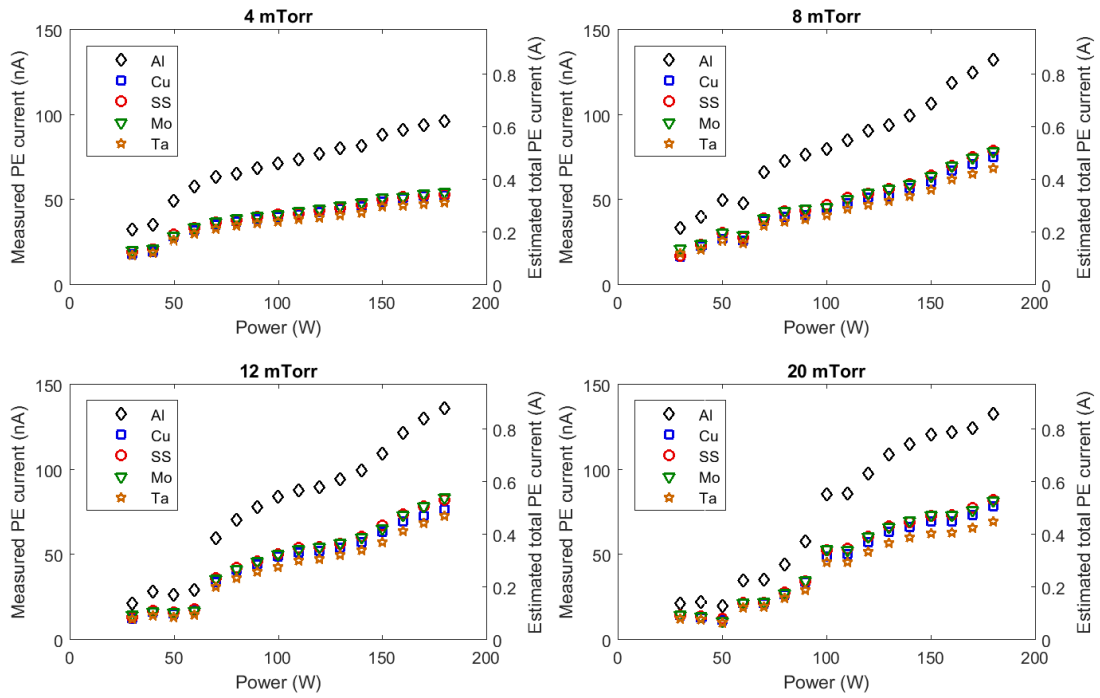


FIGURE 6. Photoelectron currents from different metal samples when the photoelectron meter is looking to the ECR zone. The power is varied in selected pressures.

work function is in the order of 4–5 eV. This is for clean surfaces, and the real work function of technical surfaces covered with their natural oxide and contaminants, typically found in ion sources, can be different. The emitted electrons are further accelerated by the plasma potential, which has been measured to be about 4–9 V (depending on the source parameters) in Prometheus I [28] and, thus, their final energies can reach approximately 15 eV. These electrons can contribute to various plasma processes, with threshold energies below 15 eV. These processes include dissociative electron attachment ($e_{\text{cold}} + \text{H}_2(X^1\Sigma_g^+; v'') \rightarrow \text{H}_2^-(^2\Sigma_u^+) \rightarrow \text{H}(1s) + \text{H}^-$) where low energy electrons (< 5 eV) are required, molecular excitation from the ground state ($X^1\Sigma_g^+; v'' = 0$) to $B^1\Sigma_u^+$ and $C^1\Pi_u^+$ singlet states (threshold energies approximately 12 eV [29]), excitation from the ground state to $a^3\Sigma_g^+$ and repulsive $b^3\Sigma_u^+$ triplet states (threshold about 12 eV and 8 eV, respectively [30]), and electron detachment ($e + \text{H}^- \rightarrow 2e + \text{H}$) which has a high cross section for energies higher than ~ 2 eV [30]. Altogether, the role of photoelectrons is not well known. For the source Prometheus I, which is characterized by an excess of vibrational states and a lack of cold electrons [28], it is possible that an additional source of electrons could only be beneficial.

There is a parametric correlation between PE emission and H^- production, as deduced from the correlation of negative ion density (by means of laser photodetachment) and VUV emission measurements under the same operating conditions [26]. This is probably due to the fact that PE emission is directly proportional to photon emission rate, which correlates to vibrational excitation and ionization. It has also been observed in probe measurements that the hot electron temperature is always about 15 eV in Prometheus I [28]. Thus, the parametric dependence of the PE emission is determined only by the variation of electron density.

ACKNOWLEDGMENTS

This work has been supported by the EU 7th framework programme “Integrating Activities – Transnational Access”, project number: 262010 (ENSAR) and by the Academy of Finland under the Finnish Centre of Excellence Programme 2012–2017 (Nuclear and Accelerator Based Physics Research at JYFL).

REFERENCES

- [1] J. Komppula and O. Tarvainen, *Phys. Plasmas* **22**, p. 103516 (2015).
- [2] J. Komppula, O. Tarvainen, S. Lätti, T. Kalvas, H. Koivisto, V. Toivanen, and P. Myllyperkiö, *AIP Conf. Proc.* **1515**, p. 66 (2013).
- [3] J. Komppula, O. Tarvainen, T. Kalvas, H. Koivisto, R. Kronholm, J. Laulainen, and P. Myllyperkiö, *J. Phys. D: Appl. Phys.* **48**, p. 365201 (2015).
- [4] U. Fantz, S. Briefi, D. Rauner, and D. Wunderlich, *Plasma Sources Sci. Technol.* **25**, p. 045006 (2016).
- [5] J. Laulainen, T. Kalvas, H. Koivisto, J. Komppula, and O. Tarvainen, *AIP Conf. Proc.* **1655**, p. 020007 (2015).
- [6] J. Bretagne, G. Delouya, C. Gorse, M. Capitelli, and M. Bacal, *J. Phys. D: Appl. Phys.* **18**, p. 811 (1985).
- [7] S. Aleiferis and P. Svarnas, *Rev. Sci. Instrum.* **85**, p. 123504 (2014).
- [8] B. Feuerbacher and B. Fitton, *J. Appl. Phys.* **43**, p. 1563 (1972).
- [9] D. H. Dowell, F. K. King, R. E. Kirby, J. F. Schmerge, and J. M. Smedley, *Phys. Rev. Accel. Beams* **9**, p. 063502 (2006).
- [10] S. Aleiferis, P. Svarnas, I. Tsiroidis, S. Béchu, M. Bacal, and A. Lacoste, *IEEE Trans. Plasma Sci.* **42**, 2828–9 (2014).
- [11] A. Lacoste, T. Lagarde, S. Béchu, Y. Arnal, and J. Pelletier, *Plasma Sources Sci. Technol.* **11**, 407–412 (2002).
- [12] S. Béchu *et al.*, *Phys. Plasmas* **20**, p. 101601 (2013).
- [13] A. McPherson, N. Rouze, W. B. Westerveld, and J. S. Risley, *Appl. Opt.* **25**, 298–310 (1986).
- [14] S. Aleiferis, J. Laulainen, P. Svarnas, O. Tarvainen, M. Bacal, and S. Béchu, In these proceedings.
- [15] J. A. Ramsey and G. F. J. Garlick, *Br. J. Appl. Phys.* **15**, p. 1353 (1964).
- [16] T. Kalvas, O. Tarvainen, J. Komppula, M. Laitinen, T. Sajavaara, H. Koivisto, A. Jokinen, and M. P. Dehnel, *AIP Conf. Proc.* **1515**, p. 349 (2013).
- [17] K. R. Kendall, M. McDonald, D. R. Moss crop, P. W. Schmor, D. Yuan, G. Dammertz, B. Piosczyk, and M. Olivo, *Rev. Sci. Instrum.* **57**, p. 1277 (1986).
- [18] C. Courteille, A. M. Bruneteau, and M. Bacal, *Rev. Sci. Instrum.* **66**, p. 2533 (1995).
- [19] T. Kuo, R. Baartman, G. Dutto, S. Hahto, J. Ärje, and E. Liukkonen, *Rev. Sci. Instrum.* **73**, p. 986 (2002).
- [20] T. Kuo, D. Yuan, K. Jayamanna, M. McDonald, R. Baartman, P. Schmor, and G. Dutto, *Rev. Sci. Instrum.* **67**, p. 1314 (1996).
- [21] W. Kraus, U. Fantz, P. Franzen, M. Fröschle, B. Heinemann, C. Martens, R. Riedl, and D. Wunderlich, *AIP Conf. Proc.* **1515**, p. 129 (2013).
- [22] R. F. Welton *et al.*, *AIP Conf. Proc.* **1097**, p. 181 (2009).
- [23] Y. An, B. Jung, and Y. S. Hwang, *Rev. Sci. Instrum.* **81**, p. 02A702 (2010).
- [24] B. L. Henke, E. M. Gullikson, and J. C. Davis, *At. Data Nucl. Data Tables* **54**, p. 181 (1993).
- [25] M. P. Seah and W. A. Dench, *Surf. Interface Anal.* **1**, p. 2 (1979).
- [26] S. Aleiferis, O. Tarvainen, P. Svarnas, M. Bacal, and S. Béchu, *J. Phys. D: Appl. Phys.* **49**, p. 095203 (2016).
- [27] V. Baglin, J. Bojko, O. Gröbner, B. Henrist, N. Hilleret, C. Scheuerlein, and M. Taborelli, Proceedings of EPAC 2000 p. 217 (2000).
- [28] S. Aleiferis, “Experimental Study of the Production of H⁻ Negative Ions by Electron Cyclotron Resonance Plasmas,” Ph.D. thesis, University of Patras, University of Grenoble 2016.
- [29] J.-S. Yoon, M.-Y. Song, J.-M. Han, S. H. Hwang, W.-S. Chang, and B. Lee, *J. Phys. Chem. Ref. Data* **37**, p. 913 (2008).
- [30] R. K. Janev, D. Reiter, and U. Samm, *Collision Processes in Low-Temperature Hydrogen Plasmas* (2003).